UCRL - 77024
PREPRINT
Conf-751108--1

LAWRENCE LIVERMORE LABORATORY
University of California/Livermore, California

INTENSE SYNCHROTRON RADIATION FROM A MAGNETICALLY COMPRESSED RELATIVISTIC ELECTRON LAYER

J. W. Shearer, D. A. Nowak, E. Garelis, and W. C. Condit

OCTOBER, 1975

THIS PAPER WAS PREPARED FOR PRESENTATION AT THE FIRST INTERNATIONAL TOPICAL CONFERENCE ON ELECTRON BEAM RESEARCH AND TECHNOLOGY, ALBUQUERQUE, NEW MEXICO
NOVEMBER 3-5, 1975

INTENSE SYNCHROTRON RADIATION FROM A MAGNETICALLY COMPRESSED RELATIVISTIC ELECTRON LAYER*

J. W. Shearer, D. A. Nowak, E. Garelis, and W. C. Condit

University of California, Lawrence Livermore Laboratory
P.O. Box 808, Livermore, CA 94550

OCTOBER, 1975

ABSTRACT

Using a simple model of a relativistic electron layer rotating in an axial magnetic field, energy gain by an increasing magnetic field and energy loss by synchrotron radiation were considered. For a typical example, initial conditions were ∿ 8 MeV electron in a ∿ 14 kG magnetic field, at a layer radius of ∿ 20 mm, and final conditions were ∿ 4 MG magnetic field ∿ 100 MeV electron layer energy at a layer radius of ∿ 1.0 mm. In the final state, the intense 1-10 keV synchrotron radiation imposes an electron energy loss time constant of ∿ 100 nanoseconds. In order to achieve these conditions in practice, the magnetic field must be compressed by an imploding conducting liner; preferably two flying rings[8] in order to allow the synchrotron radiation to escape through the midplane. The synchrotron radiation loss rate imposes a lower limit to the liner implosion velocity required to achieve a given final electron energy (∿ 1 cm/μsec in the above example). In addition, if the electron ring can be made sufficiently strong (field reversed), the synchrotron radiation would be a unique source of high intensity soft x-radiation.

*Work performed under the auspices of the United States Energy Research and Development Administration under contract No. W-7405-Eng-48.

I. INTRODUCTION

Stable layers and rings of relativistic electrons in magnetic mirror geometry have been studied for a number of years, particularly at the Lawrence Livermore Laboratory ("ASTRON")[1,2] and at Cornell University.[3] Theoretical studies have shown that these layers can be compressed to high energy by increasing the magnetic confinement field.[4,5] As the magnetic field is raised, the emission rate of synchrotron radiation by the electrons rapidly increases because of the growth of both the magnetic field and the electron energy. In this paper we shall investigate the conditions for which the electron energy loss by synchrotron radiation approaches and exceeds the energy gain from the compression. We will then discuss the experimental aspects of the maximum electron ring energy, the synchrotron radiation intensity, and the synchrotron spectrum.

II. SINGLE ELECTRON MODEL EQUATIONS

For the sake of clarity we present a single electron model for weak cylindrical layers; that is, $\nu << \gamma$, where $\nu = N'r_0$, N' = electrons per unit length, r_0 = classical electron radius, and γ is the ratio of total electron energy to rest energy mc^2. This model is also applicable to a high ν current-neutralized layer. We assume relativistic electrons ($\gamma >> 1$). Then the orbit radius a is given by:

$$a = c/\Omega_e = 1_A \gamma/B \qquad (1)$$

where Ω_e is the gyrofrequency of the electron,[1] where B is the magnetic field (unperturbed by the electrons in this approximation), and

where I_A is the Alfven current constant:

$$I_A = mc^2/e = 1700 \text{ abamp.} \tag{2}$$

The synchrotron radiation power rate P per electron is given by[6]

$$P = \frac{2}{3} \frac{ce^2}{I_A^2} \gamma^2 B^2 \tag{3}$$

We define the time constant τ_s for the fractional loss rate of energy from the electron by means of synchrotron radiation:

$$\frac{1}{\tau_s} \equiv \frac{P}{\gamma mc^2} = \frac{2}{3} \frac{ce}{I_A^3} \gamma B^2 \tag{4}$$

We will not discuss the details of the spectrum of the synchrotron radiation, but simply quote the equation for its characteristic energy E_0 and characteristic frequency ω_0.[6]

$$E_0 = \hbar\omega_0 = 3\hbar \gamma^3 \Omega_e = 3e \lambda\!\!\!^{-} \gamma^2 B \tag{5}$$

where $\lambda\!\!\!^{-} = \hbar/mc$ is the Compton wavelength of the electron. Figure 1 shows a comparison of the synchrotron spectrum[6] with that of a blackbody.

In order to compute the effect of changing the magnetic field, we consider the canonical angular momentum of the electron P_θ which can be written:[5]

$$P_\theta = -\frac{1}{2} \frac{e}{c} B a^2 \tag{6}$$

P_θ is a constant of the electron motion; using this fact, one can

derive the compression time constant τ_c from Eqs. (1) and (6):

$$\frac{1}{\tau_c} \equiv \frac{\dot{\gamma}}{\gamma} = \frac{1}{2}\frac{\dot{B}}{B} = -\frac{\dot{a}}{a} \tag{7}$$

Thus, the complete equation for the time dependence of the electron energy becomes:

$$\left.\begin{aligned} \frac{\dot{\gamma}}{\gamma} &= \frac{1}{\tau_c} - \frac{1}{\tau_s} \\ &= \frac{1}{2}\frac{\dot{B}}{B} - \frac{2}{3}\frac{ce}{I_A^3}\gamma B^2 \end{aligned}\right\} \tag{8}$$

Strictly speaking, P_θ is no longer a constant when the synchrotron loss term $1/\tau_s$ becomes large compared to the compression term $1/\tau_c$. However, as long as the fractional radiation loss per electron revolution is low ($\tau_s \Omega_e >> 1$), P_θ changes only slowly, and Eq. (8) is a sufficient approximation for our purpose.

Equation (7) shows that as the magnetic field is increased the orbit shrinks; therefore, fixed radius coils would not be an energy-efficient method of supplying the increasing magnetic field because most of the coil volume would be empty of electrons at the higher fields. Consequently, we shall assume that the magnetic field is increased by means of a moving metal liner -- a well-known method of producing megagauss magnetic fields.[7,8] We are implicitly assuming that the metallic liners will be driven by magnetic fields[8] rather than by high explosives[7] because that method appears to be more convenient and less destructive. If we neglect resistive losses in the

liner, the conservation of flux can be written:

$$B/B_0 = (R_0/R)^2 \tag{9}$$

where R is the radius of the metal liner.

Figure 2 is a plot of orbit radius a, characteristic energy E_c, and radiation loss time constant τ_s in some parameter ranges of interest. In a loss-less system, a given electron moves along a straight line of constant $\frac{\gamma^2}{B}$ (in Fig. 2) as the magnetic field is varied. Thus, a 10 MeV electron in a 10 kG magnetic field can be compressed by the liner to become a 100 MeV electron in a 1 MG field, provided the compression time τ_c is much less than the radiation loss time constant τ_s over the entire path. If $\tau_c \gtrsim \tau_s$, then Eq. (8) must be solved, and the path of the electron in Fig. 2 is curved.

III. SOME SOLUTIONS FOR THE SINGLE ELECTRON MODEL

A simple computer code was written to solve Eq. (8) under the conditions of liner compression according to Eq. (9). The liner was approximated by a "point mass" which was given an initial inward velocity $U_0 = -\dot{R}$ at the initial radius R_0. The liner was then decelerated by the magnetic pressure; however, for most of the code runs this deceleration was negligible over the compression range of interest. It was subsequently realized that the principal characteristics of these solutions could be found analytically. The analytical results are presented here; the computer output shows similar behavior.

Equation (8) can be rewritten in terms of the liner implosion velocity $U = -\dot{R}$, with the help of Eq. (9):

$$\frac{\dot{\gamma}}{\gamma} = \frac{1}{\tau_c} - \frac{1}{\tau_s} = \frac{U}{R} - \frac{1}{\tau_s} \tag{10}$$

In order to reach a required maximum value of the characteristic synchrotron energy E_0, we must have $\tau_c \leq \tau_s$ (or $\dot{\gamma} \geq 0$), which implies that the liner velocity U must satisfy:

$$U \geq \frac{R}{\tau_s} = \left(\frac{2}{9}\frac{c}{I_A^2 \lambda}\right)\left(\frac{R}{a} E_0\right) \tag{11}$$

where we have used Eqs. (1), (4), and (5). Numerically, Eq. (11) is:

$$U\ (\text{mm}/\mu\text{sec}) \geq \left(.95\ \frac{R}{a}\right) E_0\ (\text{keV}) \tag{12}$$

In practical liner systems $1 \leq (R/a) \leq 2$; thus, liner velocities of 2-20 mm/μsec correspond to synchrotron radiation in the 2-10 keV soft x-ray regime. Note that Eqs. (11) - (12) are valid at each value of E_0 over a wide range of values of γ and B given by the line of constant $E_0 = \hbar\omega_0$ plotted in Fig. 2.

Next we solve for the time-dependent solution of Eq. (10) by introducing the compression variable λ:

$$\lambda \equiv \frac{R_0}{R} = \frac{1}{1 - t/T_0} \tag{13}$$

where $T_0 \equiv R_0/U$, and where the liner wall has constant velocity U. Consider the solution of Eq. (10) in the time interval $0 \leq t < T_0$; we will never need to reach the end of this time interval at T_0 because the synchrotron radiation term always becomes dominant before

t reaches T_0. In terms of the variable λ, we have

$$\dot{\gamma} = \frac{\lambda^2}{T_0} \frac{d\gamma}{d\lambda} \tag{14a}$$

$$\frac{U}{R} = \frac{\lambda}{T_0} \tag{14b}$$

$$\frac{1}{\tau_s} = \frac{1}{\tau_{s0}} \frac{\gamma}{\gamma_0} \lambda^4 \tag{14c}$$

where τ_{s0} and γ_0 are the values of τ_s and γ at time t = 0, and where we have used Eq. (9) for the liner flux compression.

Next we substitute Eq. (14) back into Eq. (10). The resultant differential equation is then solved by means of the introduction of an intermediate variable $y = \gamma/\lambda$; we omit the algebra here, and write down the solution:

$$\frac{\gamma}{\gamma_0} = \frac{\lambda}{1 + \alpha (\lambda^4 - 1)} \tag{15}$$

where $\alpha = T_0/4\tau_{0s}$. The corresponding solutions for the characteristic synchrotron energy E_0 and radiation power P are then readily obtained:

$$\frac{E_0}{E_{00}} = \left(\frac{\lambda\gamma}{\gamma_0}\right)^2 = \frac{\lambda^4}{[1 + \alpha (\lambda^4 - 1)]^2} \tag{16}$$

$$\frac{P}{P_0} = \left(\frac{\gamma B}{\gamma_0 B_0}\right)^2 = \lambda^4 \left(\frac{\gamma}{\gamma_0}\right)^2 = \frac{\lambda^6}{[1 + \alpha (\lambda^4 - 1)]^2} \tag{17}$$

where E_{00} and P_0 are the values of E_0 and P at time t = 0, respectively.

A specific example of these solutions is given in Fig. 3, which plots the time history of the parameters B, γ, E_0, P, and a. The curves are shown as dotted lines for times when the magnetic field B

exceeds 17 megagauss, because practical liners are not likely to exceed this compression limit,[9] and the constant liner velocity assumption of the analysis is no longer realistic. However, in this example one finds that the electron energy γmc^2 and the characteristic synchrotron energy E_0 have both reached their maximum values at earlier times where the magnetic field is less than 10 megagauss and the solution is a good approximation.

If we apply Eq. (12) to the example of Fig. 3, we find that:

$$E_0 \text{ (keV)} \leq \frac{aU}{.95\ R} = \frac{a_0 \text{ (mm)}}{.95\ T_0} = 7.2 \text{ keV} \tag{18}$$

This result agrees with the 7.0 keV maximum energy plotted in Fig. 3. The corresponding liner velocity, $U = R_0/T_0$, is 8.8 mm/μsec for an initial liner radius $R_0 = 2.5$ cm. Note also that the peak of each curve in Fig. 3 occurs in the time sequence, γmc^2, E_0, and P, as expected from the form of Eq. (15), (16), and (17). Finally, we observe that the orbit radius a shrinks more rapidly than it would in the absence of synchrotron radiation.

IV. ELECTRON LAYERS AND RINGS

The single electron theory which we have just discussed is not exact for the case of an intense non-current-neutralized electron layer or ring whose self-magnetic field perturbs the initial vacuum field.[1,2,3] The effects of synchrotron radiation need to be added to the more extended treatments of magnetic compression of electron layers and rings.[4,5] In addition the variations of electron energy and path curvature within the layer would change the synchrotron rad-

iation characteristics (see Fig. 4). However, our preliminary calculations suggest that the synchrotron spectrum shape is not greatly changed for an electron layer for which $\gamma = v$.[10] Nevertheless more analysis is needed, especially because the recent Cornell experimental results[11] demonstrate that in practice most electron layer equilibria are not long cylinders, but rather doughnut or ring-like shapes.

We shall not indulge in an extensive discussion of the formation and stability of electron rings here; however, a few comments are pertinent. Relativistic synchrotron radiation is strongly peaked in the forward direction,[6] with an average angle of the order of $1/\gamma$ radians. For a single electron gyrating in a magnetic field B, this translates into a narrow cone of radiation with the cone angle θ_c given by

$$\tan \theta_c = v_\perp / v_\parallel \tag{19}$$

where $v_\perp$ and $v_\parallel$ are the electron velocities perpendicular and parallel to the magnetic field, respectively. In a practical electron ring trapped in a mirror field there is a distribution of electron velocities which spreads the synchrotron radiation out over a solid angle of about 0.1 steradian at the midplane, as diagrammed in Fig. 5. If one wishes to measure the synchrotron radiation, it is desirable to keep the midplane free from absorbing materials, such as liners. The "flying ring" imploding liner geometry[8] is suitable for this purpose, as shown in Fig. 6; it is also a simple way to keep the electron ring confined in a magnetic mirror geometry.

A choice of techniques is available for the initial formation of the electron ring. A conventional inflector and resistive layer trapping arrangement is shown in Fig. 7; more recently injection of a straight hollow beam through a magnetic cusp geometry has been successfully used to form a rotating beam from which a few percent of the electrons have been subsequently trapped as a field-reversed electron layer in a magnetic mirror.[12]

The 1.93 cm initial radius (at 13.75 kG) of our liner example (Fig. 3) is somewhat smaller than the experimental radii (at lower field) attained in recent experiments;[11,12] however, a moving magnetic mirror technique[13] can be used to transfer and compress the ring from its initial formation site into the liner structure.

V. CONCLUSIONS

We have seen that if relativistic electrons are compressed to megagauss fields, energy loss by synchrotron radiation can effectively compete with compressional energy gain. Such effects could be studied experimentally by combining relativistic electron rings with magnetically-driven liner technology.

Let us estimate the total synchrotron power loss rate for the previous example (Fig. 3); at 2.7 μsec the power P is approximately 23³ μwatts/electron. If the layer is 1 mm long, then the total number of electrons N_L in the layer is:

$$N_L = (0.1)\,\frac{\nu}{r_0} = 3.5 \times 10^{11}\,\nu \qquad (20)$$

The corresponding total power output PN_L would be approximately 83 ν megawatts, and for a power pulse half-width of about 65 nanoseconds (Fig. 3), we obtain a total radiated energy estimate of $\gtrsim 5\ \nu$ joules. Using an average electron energy at 2.7 μsec $\gamma \approx 100$, then for an electron layer where $\gamma = \nu$ (the threshold of field reversal) we obtain ~ 500 joules of synchrotron radiation. Using an angular estimate of 0.1 steradians (Fig. 5) we obtain a rough estimate of $\sim 50\nu$ joules/cm^2 of radiation at a radius of 10 cm in the midplane, which is well outside the initial radius of the liner in this example. This is a large energy flux at a short wavelength as compared to conventional accelerator-produced synchrotron sources.[14,15]

Another application of this analysis is to estimate the amount of electron energy multiplication achievable by compression. It is useful to note that the maximum electron energy is efficiently attained before the synchrotron radiation power becomes dominant (Fig. 3). Consequently, it should be possible to design an experiment to extract these high energy electrons; one would use a pair of flying ring liners where one of the rings is lighter than the other and rebounds sooner from the magnetic field pressure. At that time, the corresponding magnetic mirror would disappear and the electron ring would be projected down the axis in a time that is short compared to the compression time (in the millimeter-scale geometry of the example). For this projection process the magnetic moment $\mu = \gamma m v_\perp^2/2B$ is approximately an adiabatic

invariant;[16] therefore, without significant change in the total energy the electron ring velocity $v_\perp$ will be converted into parallel velocity $v_\parallel$ as B becomes smaller along the axis. With optimum timing of the disappearance of the weaker mirror, the example of Fig. 3 indicates that one can convert 7.75 MeV electrons into 100 MeV electrons at 2.65 μsec. Using the same total number N_L of electrons as in the previous example ($\nu \approx 100$), we find that the energy of the 100 MeV electron shower is $\sim$ 500 joules, similar to the synchrotron radiation yield previously estimated. The size, shape, and duration of this electron pulse depends on the details of the field distribution at the weaker mirror position, and will not be considered here.

Thus we conclude that liner compression of electron rings can be used to produce either $\sim$ 100 MeV pulsed electron showers or high intensity synchrotron radiation in the 1-10 keV soft x-ray region.[17]

VI. ACKNOWLEDGEMENT

We wish to thank William Lokke for his encouragement and support.

REFERENCES

1. N. C. Christofilos, W. C. Condit, T. J. Fessenden, R. E. Hester, S. Humphries, G. D. Porter, B. W. Stallard, and P. B. Weiss, in Plasma Physics and Controlled Nuclear Fusion Research, (International Atomic Energy Agency, Vienna, 1971), Vol. 1, p. 1_9.

2. R. J. Briggs, G. D. Porter, B. W. Stallard, J. Taska, and P. B. Weiss, The Physics of Fluids, Vol. 16, No. 11, p. 1934, (1973).

3. J. J. Bzura, T. J. Fessenden, H. H. Fleischmann, D. A. Phelps, A. C. Smith, Jr., and D. M. Woodall, Physical Review Letters, Vol. 29, No. 5, p. 256, (1972).

4. George Schmidt, Physical Review Letters, Vol. 26, No. 16, p. 952, (1971).

5. George Schmidt, The Physics of Fluids, Vol. 15, No. 8, p. 1540, (1972).

6. J. D. Jackson, Classical Electrodynamics, (John Wiley & Sons, New York, 1962), p. 471 ff.

7. C. M. Fowler, Science, Vol. 180, p. 261, (1973).

8. A. E. Robson, Proceedings of the Conference on Electrostatic and Electromagnetic Confinement of Plasmas and the Phenomenology of Relativistic Electron Beams, Annals of the New York Academy of Sciences, Volume 251, New York (1975), p. 649.

9. H. Knoepfel, Pulsed High Magnetic Fields, North-Holland Publishing Company, Amsterdam, (1970), pp. 216-219.

10. D. A. Nowak, Effects of Synchrotron Radiation on the Compression of a Relativistic Electron Layer, U. of Calif., Lawrence Livermore Laboratory Report UCID-16689, (1975).

11. D. A. Phelps, A. C. Smith, D. M. Woodall, R. M. Meger, and H. H. Fleischmann, The Physics of Fluids, Vol. 17, p. 2226, (1974).

12. R. E. Kribel, K. Shinsky, D. A. Phelps, and H. H. Fleischmann, Plasma Physics, Vol. 16, p. 113, (1974).

13. H. H. Fleischmann, p. 472 of Ref. 8.

14. M. L. Perlman, E. M. Rowe, and R. F. Watson, "Synchrotron Radiation-Light Fantastic", Physics Today, Vol. 27, No. 7, p. 30, (1974).

15. M. N. Yakimenko, Usp. Fiz. Nauk. 114, 55-66 (Sept. 1974) [Engl. Trans. Sov. Phys. - Usp. 17, 651-657 (1975)].

16. L. Spitzer, The Physics of Fully Ionized Gases, 2nd ed., Interscience, New York, p. 13, (1962).

17. W. C. Condit and D. A. Nowak, "Suggestions for a Submicrosecond Soft X-Ray Source", U. of Calif., Lawrence Livermore Laboratory Report UCID-16611-1, (1975).

FIGURE LEGENDS

Figure 1

Intensity-normalized spectra of synchrotron and black body radiation plotted against log frequency. Note that the peaks were aligned by setting (3/2) kT = (1/4) $\hbar\omega$.

Figure 2

Selected values of orbit radius a [Eq. (1)], characteristic synchrotron energy E_0 [Eq. (5)], and synchrotron radiation loss time constant τ_s [Eq. (4)] are plotted versus magnetic field B and electron energy $mc^2\gamma$.

Figure 3

Numerical value of synchrotron power P (microwatts/electron), electron energy γmc^2 (MeV), characteristic synchrotron energy E_0 (keV), magnetic field B (megagauss), and orbit radius a (mm) plotted versus time t (microseconds) at late times for an example for which $\gamma_0 = 15.5$, $B_0 = 13.75$ kG, $a_0 = 19.32$ mm, $T_0 = 2.828$ μsec, and $\alpha = 4.0 \times 10^{-6}$.

Figure 4

Radial Betatron Oscillations: We have assumed a field-reversed layer so the trajectories have negative curvature inside the orbit.

Figure 5

Effect of axial betatron oscillations on synchrotron emission angle.

Figure 6

"Flying ring" moving metal liners compressing a relativistic electron ring.

Figure 7

Injection and trapping of relativistic electron layers.

Figure 1

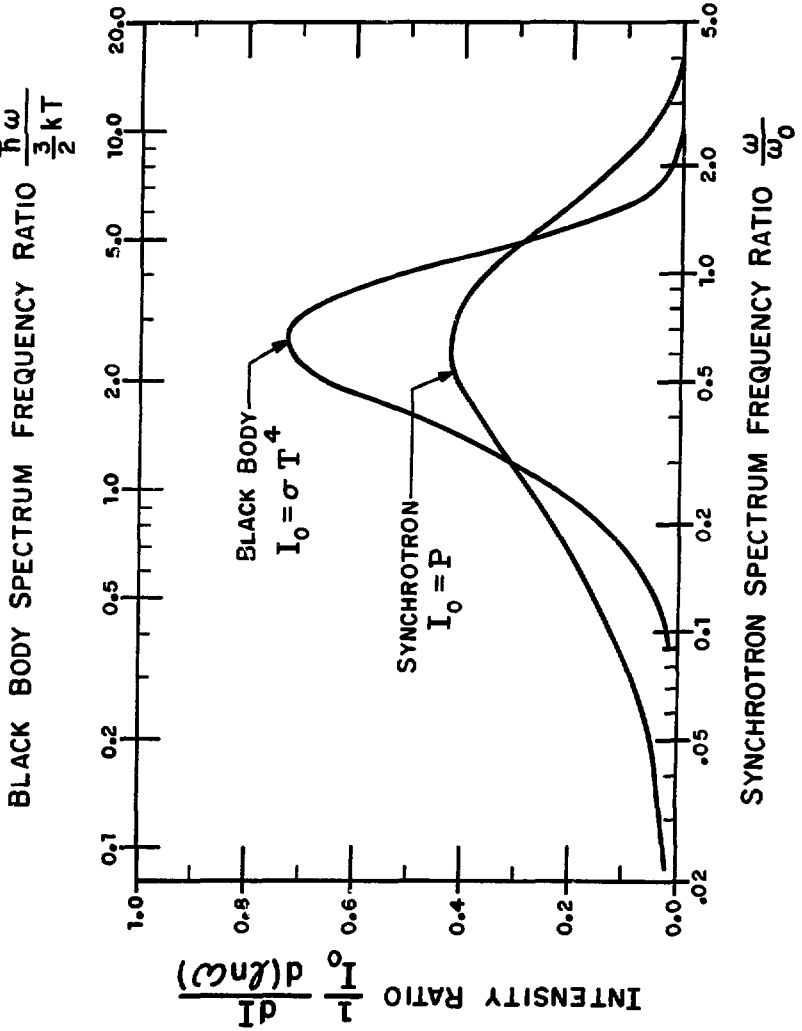
BLACK BODY SPECTRUM FREQUENCY RATIO $\frac{\hbar\omega}{\frac{3}{2}kT}$
SYNCHROTRON SPECTRUM FREQUENCY RATIO $\frac{\omega}{\omega_0}$
INTENSITY RATIO $\frac{1}{I_0}\frac{dI}{d(\hbar\omega)}$
BLACK BODY
$I_0 = \sigma T^4$
SYNCHROTRON
$I_0 = P$
20.0
10.0
5.0
2.0
1.0
0.5
0.2
0.1
5.0
2.0
1.0
0.5
0.2
0.1
.05
.02
1.0
0.8
0.6
0.4
0.2
0.0

Figure 2

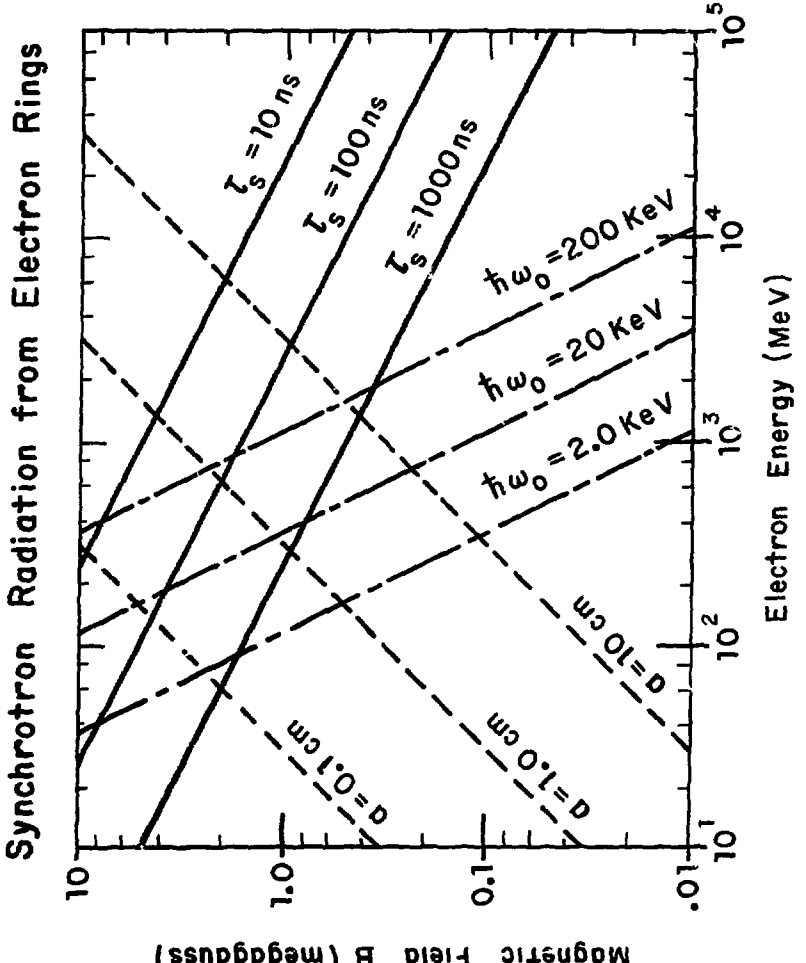
Synchrotron Radiation from Electron Rings
Magnetic Field B (megagauss)
Electron Energy (MeV)
10
1.0
0.1
.01
10^1
10^2
10^3
10^4
10^5
τ_s = 10 ns
τ_s = 100 ns
τ_s = 1000 ns
$\hbar\omega_0$ = 200 KeV
$\hbar\omega_0$ = 20 KeV
$\hbar\omega_0$ = 2.0 KeV
D = 10 cm
D = 1.0 cm
D = 0.1 cm

Figure 3

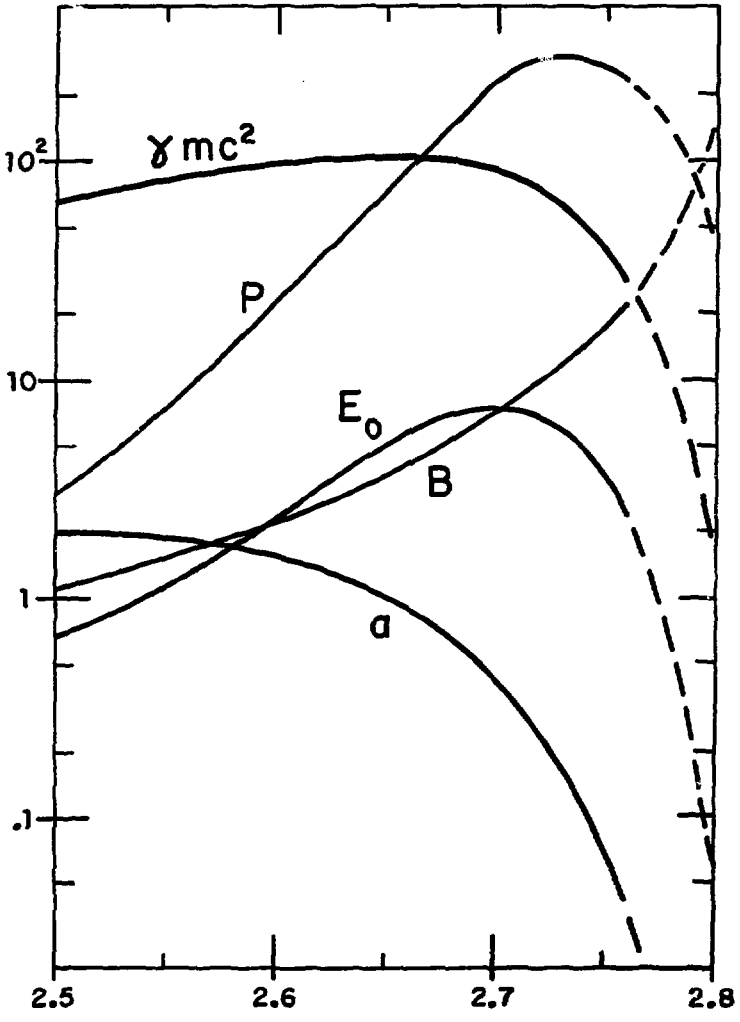

Figure 4

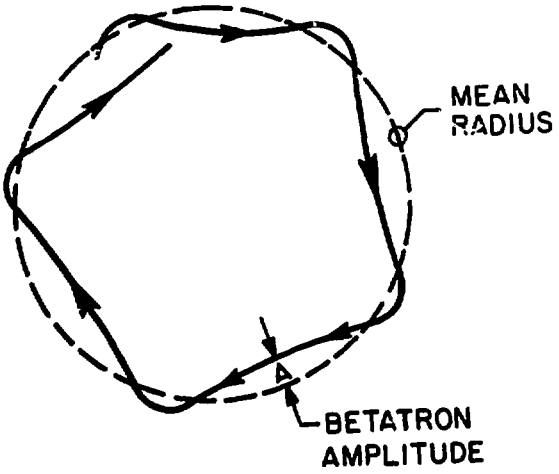

Figure 5

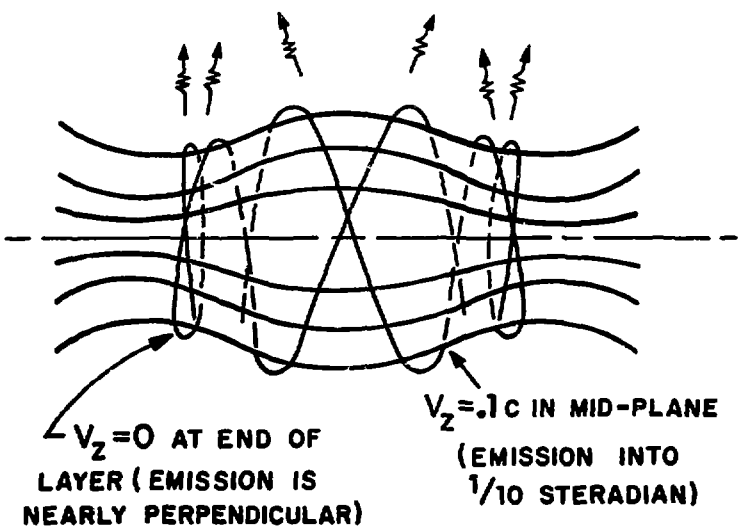
V_z=0 AT END OF LAYER (EMISSION IS NEARLY PERPENDICULAR)
V_z=.1c IN MID-PLANE (EMISSION INTO 1/10 STERADIAN)

Figure 6

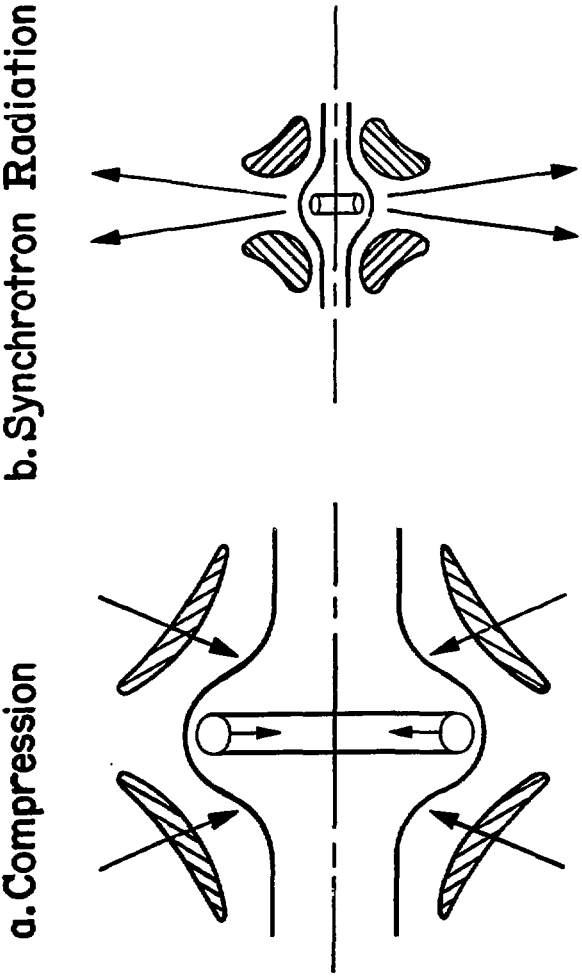

Figure 7

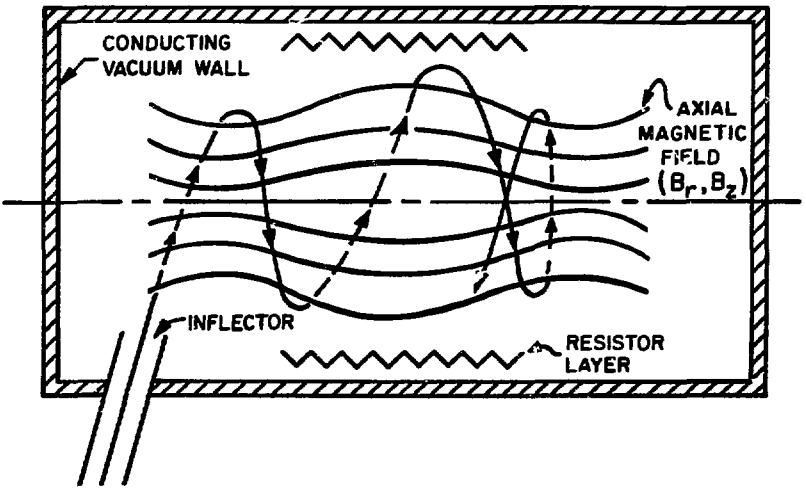
CONDUCTING
VACUUM WALL
AXIAL
MAGNETIC
FIELD
(B_r, B_z)
INFLECTOR
RESISTOR
LAYER